

Resonant and Non-Resonant Modulated Amplitude Waves for Binary Bose-Einstein Condensates in Optical Lattices

Mason A. Porter¹, P.G. Kevrekidis² and B.A. Malomed³

¹*School of Mathematics and Center for Nonlinear Science, Georgia Institute of Technology, Atlanta GA 30332, USA*

²*Department of Mathematics and Statistics, University of Massachusetts, Amherst MA 01003-4515, USA*

³*Department of Interdisciplinary Studies, Faculty of Engineering, Tel Aviv University, Tel Aviv 69978, Israel*
(October 26, 2019)

We consider a system of two Gross-Pitaevskii (GP) equations, in the presence of an optical-lattice (OL) potential, coupled by both nonlinear and linear terms. This system describes a Bose-Einstein condensate (BEC) composed of two different spin states of the same atom which interact linearly through a resonant electromagnetic field. In the absence of the OL, plane-wave solutions are found, and their stability is examined. In the presence of the OL, we derive a system of amplitude equations for spatially modulated states which are coupled to the periodic potential through the lowest-order subharmonic resonance. We determine this system's equilibria, which represent spatially periodic solutions and subsequently examine stability of the corresponding solutions by direct simulations of the coupled GP equations. We find that symmetric (equal amplitude) and asymmetric (unequal amplitude) dual-mode resonant states are, respectively, stable and unstable. The unstable state generates periodic oscillations between the two components, which is possible only due to the linear coupling between them. Four-mode states are also found, but they are always unstable.

PACS: 05.45.-a, 03.75.Lm, 05.30.Jp, 05.45.Ac

I. INTRODUCTION

At low temperatures, particles in a dilute boson gas can fall in the same (ground) state, forming a Bose-Einstein condensate (BEC). This was first observed experimentally in 1995 in Na and Rb vapors [34,16,24,11].

In the mean-field approximation, a dilute BEC is described by the nonlinear Schrödinger (NLS) equation with an external potential, which is also called the Gross-Pitaevskii (GP) equation. In particular, BECs may be considered in the quasi-one-dimensional (quasi-1D) regime, with the transverse dimensions of the condensate on the order of its mean healing length χ and a much larger longitudinal dimension [8,9,7,16]. The length χ is determined by the mean atomic density n and the two-body s -wave scattering length a (where interactions between atoms are repulsive if $a > 0$ and attractive if $a < 0$), $\chi^2 = (8\pi n|a|)^{-1}$ [34,16,25,4].

In the quasi-1D regime, which corresponds to “cigar-shaped” BECs, one employs the 1D limit of the 3D mean-field description, rather than a true 1D mean-field theory (which would be appropriate for extremely small transverse dimensions, $\sim a$) [8,7,9,42,5]. Then, the condensate wave function $\psi(x, t)$ obeys the 1D GP equation,

$$i\hbar\psi_t = -\frac{\hbar^2}{2m}\psi_{xx} + g|\psi|^2\psi + V(x)\psi, \quad (1)$$

where m is the atomic mass, $V(x)$ is an external potential, and $g = [4\pi\hbar^2 a/m][1 + O(\mu^2)]$, where $\mu = \sqrt{n|a|^3}$ is the dilute-gas parameter [16,25,4,26]. Relevant potentials $V(x)$ include harmonic traps and periodic potentials (optical lattices, OLs). In the case of quasi-1D cylindrical (“cigar-shaped”) BECs,

$$V(x) = V_0 \cos[2\kappa(x - x_0)] + \frac{1}{2}V_1 x^2, \quad (2)$$

where x_0 is the offset of the periodic potential relative to the center of the the parabolic trap. When $(2\pi/\kappa)^2 V_1 \ll V_0$, the potential is dominated by its periodic component over many periods [17,13,10]; for example, when $V_0/V_1 = 500$ and $\kappa = 10$, the parabolic component in $V(x)$ is negligible for 10 periods. In this work, we set $V_1 = 0$ and focus on periodic potentials, which have been employed in numerous recent experimental studies of BECs [21,3], and have also received intense theoretical attention [8,7,9,6,15,13,17,31,2,44,36,35,32,46,28,27].

Coupled BECs, which constitute the subject of this work, were considered in several theoretical works [22,38,37,19,12,43,18]. In the case of nonlinear interaction between two different species (such as ⁸⁵Rb and ⁸⁷Rb), the

simplest model is

$$\begin{aligned} i\hbar \frac{\partial \psi_1}{\partial t} &= -\frac{\hbar^2}{2m_1} \nabla^2 \psi_1 + g_1 |\psi_1|^2 \psi_1 + V(x) \psi_1 + h |\psi_2|^2 \psi_1, \\ i\hbar \frac{\partial \psi_2}{\partial t} &= -\frac{\hbar^2}{2m_2} \nabla^2 \psi_2 + g_2 |\psi_2|^2 \psi_2 + V(x) \psi_2 + h |\psi_1|^2 \psi_2, \end{aligned} \quad (3)$$

where $m_{1,2}$ are the masses of the species, $g_j = 4\pi\hbar^2 a_j / m_j$ corresponds to the (self-)scattering length a_j , and

$$h \equiv g_{12} = 2\pi\hbar^2 a_{12} (m_1 + m_2) / (m_1 m_2) \quad (4)$$

corresponds to the cross-scattering length a_{12} [38]. There are numerous subcases of Eqs. (3) to consider, as various combinations of signs for the scattering coefficients g_1 , g_2 , and h may occur. It is important to note, however, that if $g_{1,2}$ are positive (repulsion between the atoms), then h must, typically, be positive too. If $g_{1,2}$ are negative, h [see Eq. (4)] may be *either* positive or negative.

The system (3) resembles a well-known model that describes the nonlinear self-phase-modulation (SPM) and cross-phase-modulation (XPM) interactions of light waves with different polarizations or carried by different wavelengths [1] in nonlinear optics. In the case of optical fibers, the evolution variable is the propagation distance z rather than the time t , and the role of x is played by the reduced temporal variable τ [1]. In optical models, however, the choice of the nonlinear coefficients is limited to the combinations $g_1 = g_2 = 3h/2$ for orthogonal linear polarizations in a birefringent fiber, and $g_1 = g_2 = h/2$ for circular polarizations or different carrier wavelengths. Actually, the latter case is quite important (although, strictly speaking, it is only a special case) in the application to two-component BECs as well, as it occurs if one assumes that the collision lengths for interactions between all the atoms are the same.

Another physically interesting feature is linear coupling between two different hyperfine states of the same species of atoms, which can be induced by a resonant microwave field driving the mixture. For example, two different spin states of ^{87}Rb have been created in the same trap using sympathetic cooling [33]. The normalized coupled GP equations in this situation take the form

$$\begin{aligned} i \frac{\partial \psi_1}{\partial t} &= -\nabla^2 \psi_1 + g |\psi_1|^2 \psi_1 + V(x) \psi_1 + h |\psi_2|^2 \psi_1 + \alpha \psi_2, \\ i \frac{\partial \psi_2}{\partial t} &= -\nabla^2 \psi_2 + g |\psi_2|^2 \psi_2 + V(x) \psi_2 + h |\psi_1|^2 \psi_2 + \alpha \psi_1, \end{aligned} \quad (5)$$

where the self- and cross-scattering coefficients are g and h , and the linear coupling coefficient is α , which can always be made positive without loss of generality.

The model combining nonlinear XPM and linear couplings, as in Eqs. (5), occurs in fiber optics as well. In that case, the linear coupling is generated by a twist applied to the fiber in the case of two linear polarizations, or by an elliptic deformation of the fiber's core in the case of circular polarizations (see, for example, [29]). When considering different wavelengths, linear coupling is impossible. Another optical model, with only linear coupling between two modes, applies to dual-core nonlinear fibers, as discussed in [30] (and references therein). In the context of BECs, it may correspond to a special case in which the cross-scattering length is made (very close to) zero using a Feshbach resonance [23].

In this work, we aim to investigate modulated-wave states in the binary BEC described by Eqs. (5), which include both the nonlinear and linear couplings. First, we set the stage by examining plane-wave solutions with $V(x) \equiv 0$. When $V(x) \neq 0$, we apply a standing-wave ansatz to Eq. (5), which yields parametrically forced coupled nonlinear Mathieu equations describing the spatial evolution of the fields.

By averaging over this dynamical system's slowly-varying degrees-of-freedom [41,39], we study its periodic orbits (called "modulated amplitude waves" and denoted MAWs), and test their stability (and ensuing dynamics, in the case of instability) by numerical simulations of the coupled GP equations. The dynamical behavior of such MAWs determines the spatial resonance (band) structure of this system. We consider both the non-resonant case and 2:1:1 (subharmonic) resonances. Note that the latter situation pertains to period-doubled states in BECs [27,14,36,35].

An alternative (but less general) approach to the study of binary BECs with linear coupling would be to derive exact elliptic-function solutions to Eqs. (5) for the case of elliptic-function potentials, $V(x) = -V_0 \text{sn}^2(\kappa x, k)$, as has been done for nonlinearly coupled BECs [18]. In that work, stable standing-wave solutions were found only in BECs without the linear coupling for situations in which all the interactions are repulsive.

We structure our presentation as follows: In section II, we derive plane-wave solutions and analyze their stability. In section III, we introduce modulated amplitude waves, and in section IV we derive and solve averaged equations that

describe them in both the non-resonant and resonant situations. We corroborate our results and test the stability of the MAWs using numerical simulations. Finally, in section V, we summarize our findings and present our conclusions.

II. PLANE-WAVE SOLUTIONS

In the absence of the external potential, $V = 0$, we find plane-wave solutions of the form

$$\psi_j = R_j \exp[i(k_j x - \omega_j t)], \quad j = 1, 2. \quad (6)$$

For the linearly coupled GP equation (5), it is necessary that $k_1 = k_2 \equiv k$ and $\omega_1 = \omega_2 \equiv \omega$. On the other hand, in the absence of the linear coupling, as in Eqs. (3), one may seek a broader class of solutions with independent frequencies. The results obtained in the study of optical models suggest that the linear coupling leads to very different dynamical behaviors [29].

Inserting Eq. (6) into Eqs. (5) yields

$$\begin{aligned} \omega R_1 &= k^2 R_1 + g R_1^3 + h R_1 R_2^2 + \alpha R_2, \\ \omega R_2 &= k^2 R_2 + g R_2^3 + h R_1^2 R_2 + \alpha R_1, \end{aligned}$$

which implies that

$$[(g - h)R_1 R_2 - \alpha][R_1^2 - R_2^2] = 0,$$

from which it follows that there are two possibilities:

$$R_1 = \pm R_2; \quad (7)$$

$$R_1 R_2 = \frac{\alpha}{g - h}. \quad (8)$$

With Eq. (7), a nonzero solution is $R_2 = \pm \sqrt{(k^2 + \omega \mp \alpha)/(g + h)}$. It exists when $g + h > 0$, provided that $k^2 + \omega \mp \alpha > 0$, and when $g + h < 0$, if $k^2 + \omega \mp \alpha < 0$. When $g = -h$, one obtains solutions of the form $(R_1, R_2) = (\pm R, R)$ with arbitrary R , with $k^2 = \omega \mp \alpha$.

From Eq. (8), one finds that

$$R_2^2 = \frac{\omega - k^2}{2g} \pm \frac{1}{2} \sqrt{\left(\frac{\omega - k^2}{g}\right)^2 - \frac{4\alpha^2}{(g - h)^2}}, \quad (9)$$

under the restriction that this expression must be positive. When $\alpha \neq 0$, the term inside the square root is smaller in magnitude than the one outside, so solutions of this type exist as long as $(\omega - k^2)g \geq 0$ and the argument of the square root in (9) is non-negative. Hence, for repulsive and attractive BECs, the first condition implies, respectively, $\omega > k^2$ and $\omega < k^2$. When $h = 0$, Eq. (9) takes the form

$$R_2^2 = (2g)^{-1} \left(\omega - k^2 \pm \sqrt{(\omega - k^2)^2 - 4\alpha^2} \right).$$

For $h = 0$ and $h = 2g$, the condition on the argument of the square root implies that to obtain real solutions, it is necessary to impose the condition $|\omega - k^2| \geq 2\alpha$.

To examine the stability of the plane waves, we substitute

$$\psi_j(x, t) = \phi_j(x, t)[1 + \epsilon_j(x, t)], \quad |\epsilon_j|^2 \ll 1,$$

into Eqs. (5). This yields coupled linearized equations for $\epsilon_1(x, t)$ and $\epsilon_2(x, t)$. Assuming that ϵ_j is periodic in x , it can be expanded in a Fourier series,

$$\epsilon_j(x, t) = \sum_{n=-\infty}^{\infty} \hat{\epsilon}_{jn}(t) \exp(i\nu_n x),$$

where the n th mode has wave number ν_n . The perturbation growth rates that determine the stability of the n th mode are then given by

$$\lambda_n = -2ik\nu_n \pm \nu_n \sqrt{-\nu_n^2 - g(|R_1|^2 + |R_2|^2) \pm \sqrt{g^2(|R_1|^2 - |R_2|^2)^2 + 4h^2|R_1|^2|R_2|^2}}, \quad (10)$$

where the two sign combinations \pm are independent (so there are four distinct eigenvalues). Instability occurs when the quantity inside the square root in Eq. (10) has a positive real part, causing the side-band modes $k + \nu_n$, $k - \nu_n$ of the perturbed solution to grow exponentially. This can occur in the single-component condensates only for $g < 0$ [45].

Eigenvalues whose interior square root in Eq. (10) has a $+$ sign will produce the instability before ones with a $-$ sign, so we only need to check the former case. For example, if $h = 2g$, the instability occurs if

$$\nu_n^2 + g \left(|R_1|^2 + |R_2|^2 - \sqrt{|R_1|^4 + 14|R_1^2 R_2^2| + |R_2|^2} \right) < 0. \quad (11)$$

Stability conditions for the plane-wave solutions to Eqs. (5) with $V = 0$ can be obtained for all the possible sign combinations of g and h . We do not display them here, as they are rather cumbersome to write (yet straightforward to compute).

III. MODULATED AMPLITUDE WAVES

We now introduce solutions to Eqs. (5) that describe coherent structures of the form

$$\psi_j(x, t) = R_j(x) \exp[i(\theta(x) - \omega t)], \quad j = 1, 2. \quad (12)$$

Inserting Eq. (12) into Eqs. (5) and equating real and imaginary parts of the resulting equation yields

$$\begin{aligned} \omega R_1 &= -R_1'' + (\theta')^2 + gR_1^3 + V(x)R_1 + hR_2^2 R_1 + \alpha R_2, \\ \omega R_2 &= -R_2'' + (\theta')^2 + gR_2^3 + V(x)R_2 + hR_1^2 R_2 + \alpha R_1, \end{aligned} \quad (13)$$

$$\begin{aligned} 0 &= R_1 \theta'' + R_1' \theta', \\ 0 &= R_2 \theta'' + R_2' \theta', \end{aligned} \quad (14)$$

where the prime stands for d/dx . Equations (14) imply that

$$\theta(x) = c_1 \int \frac{dx'}{R_1^2(x')} = c_2 \int \frac{dx'}{R_2^2(x')}, \quad (15)$$

with arbitrary integration constants c_1 and c_2 , so $R_1(x) = bR_2(x)$ for some constant b unless $c_1 = c_2 = 0$. In other words, $R_1(x)$ and $R_2(x)$ are different in this context only when one considers solutions with null ‘‘angular momenta.’’ In the latter situation, Eqs. (13) assume the form

$$\begin{aligned} R_1' &= S_1, \\ S_1' &= -\omega R_1 + gR_1^3 + hR_1 R_2^2 + \alpha R_2 + V(x)R_1, \\ R_2' &= S_2, \\ S_2' &= -\omega R_2 + gR_2^3 + hR_1^2 R_2 + \alpha R_1 + V(x)R_2. \end{aligned} \quad (16)$$

When $V(x)$ is sinusoidal, Eqs. (16) are (linearly and nonlinearly) coupled cubic Mathieu equations.

IV. AVERAGED EQUATIONS AND SPATIAL SUBHARMONIC RESONANCES

To achieve some understanding of the band structure (spatial resonances) of the linearly coupled BECs, we average equations (16) in the physically relevant case of the harmonic OL potential,

$$V(x) = V_0 \cos(2\kappa x). \quad (17)$$

Defining $V_0 \equiv -\epsilon\tilde{V}_0$, $g \equiv \epsilon\tilde{g}$, $h \equiv \epsilon\tilde{h}$, and $\alpha \equiv \epsilon\tilde{\alpha}$, Eqs. (16) may be written as

$$\begin{aligned} R_1'' + \omega R_1 &= -\epsilon\tilde{V}_0 R_1 \cos(2\kappa x) + \epsilon\tilde{g}R_1^3 + \epsilon\tilde{h}R_1R_2^2 + \epsilon\tilde{\alpha}R_2, \\ R_2'' + \omega R_2 &= -\epsilon\tilde{V}_0 R_2 \cos(2\kappa x) + \epsilon\tilde{g}R_2^3 + \epsilon\tilde{h}R_1^2R_2 + \epsilon\tilde{\alpha}R_1. \end{aligned} \quad (18)$$

Assuming $\omega > 0$, we insert the ansatz

$$\begin{aligned} R_j(x) &= A_j(x) \cos(\sqrt{\omega}x) + B_j(x) \sin(\sqrt{\omega}x), \\ R_j'(x) &= -\sqrt{\omega}A_j(x) \sin(\sqrt{\omega}x) + \sqrt{\omega}B_j(x) \cos(\sqrt{\omega}x) \end{aligned} \quad (19)$$

(with $j = 1, 2$) into Eqs. (18). Differentiating the first equation of (19) and equating it with the second gives a consistency condition,

$$A_j' \cos(\sqrt{\omega}x) + B_j' \sin(\sqrt{\omega}x) = 0, \quad j = 1, 2, \quad (20)$$

that must be satisfied for this procedure to be valid. Inserting these equations into Eqs. (18) yields a set of coupled differential equations for A_j and B_j , whose right-hand sides are expanded as truncated Fourier series to isolate contributions from different harmonics [41,39]. The leading contribution in these equations is of $O(\epsilon)$, so the equations assume a general form

$$\begin{aligned} A_j' &= \epsilon F_{A_j}(A_1, A_2, B_1, B_2, x) + O(\epsilon^2), \\ B_j' &= \epsilon F_{B_j}(A_1, A_2, B_1, B_2, x) + O(\epsilon^2). \end{aligned} \quad (21)$$

When $\epsilon = 0$, Eqs. (18) decompose into two uncoupled harmonic oscillators. We have computed the exact functions F_{A_j} and F_{B_j} in Eqs. (21), but the expressions are rather cumbersome, so we show them only in the Appendix.

Our objective is to isolate the parts of the functions $A_j(x)$ and $B_j(x)$ that vary slowly in comparison with the fast oscillations of $\cos(\sqrt{\omega}x)$ and $\sin(\sqrt{\omega}x)$ and to derive averaged equations governing their slow evolution. To commence averaging, we decompose A_j and B_j into the sum of the slowly varying parts and small rapidly oscillating terms (which are written as power-series expansions in ϵ):

$$\begin{aligned} A_j &= \bar{A}_j + \epsilon W_{A_j}(\bar{A}_1, \bar{A}_2, \bar{B}_1, \bar{B}_2, x) + O(\epsilon^2), \\ B_j &= \bar{B}_j + \epsilon W_{B_j}(\bar{A}_1, \bar{A}_2, \bar{B}_1, \bar{B}_2, x) + O(\epsilon^2). \end{aligned} \quad (22)$$

Here, the *generating functions* W_{A_j} , W_{B_j} are chosen so as to eliminate all the rapidly oscillating terms in Eqs. (21) after the substitution of Eqs. (22).

This procedure yields evolution equations for the averaged quantities \bar{A}_j and \bar{B}_j [41], which we henceforth denote simply as A_j and B_j (all other parts from the originally defined A_j and B_j are cancelled out by the choice of the generating functions). As we shall see, the slow-flow equations so derived are different in resonant and non-resonant situations.

A. The Non-Resonant Case

When $\sqrt{\omega} \neq \kappa$ [recall that κ is half the wave number of the OL potential; see Eq. (17)], which is the non-resonant case, effective equations governing the slow evolution are

$$\begin{aligned} A_1' &= \frac{\epsilon}{\sqrt{\omega}} \left[-\frac{3\tilde{g}}{8}B_1(A_1^2 + B_1^2) - \frac{\tilde{\alpha}}{2}B_2 - \frac{\tilde{h}}{4}A_1A_2B_2 - \frac{\tilde{h}}{8}B_1(A_2^2 + 3B_2^2) \right] + O(\epsilon^2), \\ A_2' &= \frac{\epsilon}{\sqrt{\omega}} \left[-\frac{3\tilde{g}}{8}B_2(A_2^2 + B_2^2) - \frac{\tilde{\alpha}}{2}B_1 - \frac{\tilde{h}}{4}A_1A_2B_1 - \frac{\tilde{h}}{8}B_2(A_1^2 + 3B_1^2) \right] + O(\epsilon^2), \\ B_1' &= \frac{\epsilon}{\sqrt{\omega}} \left[\frac{3\tilde{g}}{8}A_1(A_1^2 + B_1^2) + \frac{\tilde{\alpha}}{2}A_2 + \frac{\tilde{h}}{4}A_2B_1B_2 + \frac{\tilde{h}}{8}A_1(3A_2^2 + B_2^2) \right] + O(\epsilon^2), \\ B_2' &= \frac{\epsilon}{\sqrt{\omega}} \left[\frac{3\tilde{g}}{8}A_2(A_2^2 + B_2^2) + \frac{\tilde{\alpha}}{2}A_1 + \frac{\tilde{h}}{4}A_1B_1B_2 + \frac{\tilde{h}}{8}A_2(3A_1^2 + B_1^2) \right] + O(\epsilon^2). \end{aligned} \quad (23)$$

In this non-resonant case, the OL does not contribute to $O(\epsilon)$ terms, so the terms explicitly written in Eqs. (23) correspond to what one would obtain from coupled Duffing equations, as Eqs. (18) reduce to coupled Duffing oscillators in the absence of the OL [40]. These contributions yield the wave number-amplitude relations for decoupled condensates [36,35] as well as mode-wave number relations produced by the coupling terms [41].

Equations (23) give rise to three types of equilibrium points, at which $A'_1 = A'_2 = B'_1 = B'_2 = 0$: the trivial (zero) equilibrium and those which we will call double modes and quadruple modes. These will have, respectively, two and four nonzero amplitudes A_j, B_j . Single-mode and triple-mode equilibria do not exist. Different double modes that can be found are $\pi/2$ phase shifts of each other: these are A_1A_2 equilibria, with $A_1, A_2 \neq 0$ and $B_1 = B_2 = 0$, and B_1B_2 equilibria, with $A_1 = A_2 = 0$ and $B_1, B_2 \neq 0$.

The A_1A_2 equilibria satisfy

$$A_1^2 = A_2^2 = \mp \frac{4\alpha}{3(g+h)}, \quad (24)$$

where the signs $-$ and $+$ arise, respectively, when $(g+h) < 0$, and $(g+h) > 0$ (recall that $\alpha > 0$). We also compute that $A_1 = A_2$ in the former case and $A_1 = -A_2$ in the latter case. This yields the following two A_1A_2 equilibria:

$$\begin{aligned} (A_1, A_2, B_1, B_2) &= \pm \left(\sqrt{\frac{4\alpha}{3(g+h)}}, -\sqrt{\frac{4\alpha}{3(g+h)}}, 0, 0 \right), \quad \text{if } g+h > 0; \\ (A_1, A_2, B_1, B_2) &= \pm \left(\sqrt{\frac{-4\alpha}{3(g+h)}}, \sqrt{\frac{-4\alpha}{3(g+h)}}, 0, 0 \right), \quad \text{if } g+h < 0. \end{aligned} \quad (25)$$

Analogous expressions for the B_1B_2 equilibria are obtained by phase-shifting the A_1A_2 modes by $\pi/2$.

We have examined the stability of approximate stationary solutions corresponding to the double-mode equilibria obtained above, running direct simulations of the coupled GP equations (5). Typically, the simulations generate solutions that oscillate in time (as the initial configurations are definitely not exact stationary solutions) without developing any apparent instability.

One can also find four sets of quadruple-mode equilibria in which $A_1^2 = A_2^2$ and $B_1^2 = B_2^2$. In the first two sets, A_2 is arbitrary:

$$\begin{aligned} (A_1, A_2, B_1, B_2) &= \pm \left(-A_2, A_2, \pm \sqrt{-A_2^2 + \frac{4\alpha}{3(g+h)}}, \mp \sqrt{-A_2^2 + \frac{4\alpha}{3(g+h)}} \right), \quad \text{if } g+h > 0, \\ (A_1, A_2, B_1, B_2) &= \pm \left(A_2, A_2, \pm \sqrt{-A_2^2 - \frac{4\alpha}{3(g+h)}}, \pm \sqrt{-A_2^2 - \frac{4\alpha}{3(g+h)}} \right), \quad \text{if } g+h < 0. \end{aligned} \quad (26)$$

In the second two sets, B_2 is arbitrary:

$$\begin{aligned} (A_1, A_2, B_1, B_2) &= \pm \left(\pm \sqrt{-B_2^2 + \frac{4\alpha}{3(g+h)}}, \mp \sqrt{-B_2^2 + \frac{4\alpha}{3(g+h)}}, -B_2, B_2 \right), \quad \text{if } g+h > 0, \\ (A_1, A_2, B_1, B_2) &= \pm \left(\pm \sqrt{-B_2^2 - \frac{4\alpha}{3(g+h)}}, \pm \sqrt{-B_2^2 - \frac{4\alpha}{3(g+h)}}, B_2, B_2 \right), \quad \text{if } g+h < 0. \end{aligned} \quad (27)$$

Each of the expressions (26) and (27) includes four equilibria, as there are two possible sign choices. The presence of the arbitrary amplitudes in these expressions means that the quadruple-mode stationary solutions are obtained, in fact, as a rotation of the above double-mode ones, given by Eqs. (25), and by a $\pi/2$ phase shift thereof. Accordingly, direct simulations of Eqs. (5), starting with the approximate quadruple-mode stationary states, reveal only oscillations but no instability growth, just as with simulations initiated by the approximated dual-mode stationary solutions.

B. Subharmonic Resonances

The most fundamental spatial resonance is a subharmonic one, of the type 2:1:1 [41,39,20]. In this situation, the parameter ω from the initial plane-wave approximation (6) (recall that $\omega_1 = \omega_2 \equiv \omega$ in it) is assumed to be

$$\omega = \kappa^2 + \epsilon \tilde{\omega}_1 + O(\epsilon^2), \quad (28)$$

where $\epsilon\tilde{\omega}_1$ is the *detuning* parameter [39,41,40] [recall that ϵ is a small parameter; we assume $\tilde{\omega}_1 = O(1)$]. In this situation, new terms occur in Eqs. (23). The eventual result is

$$\begin{aligned}
A'_1 &= \frac{\epsilon}{\kappa} \left[\left(\frac{\tilde{\omega}_1}{2} - \frac{\tilde{V}_0}{4} \right) B_1 - \frac{3\tilde{g}}{8} B_1 (A_1^2 + B_1^2) - \frac{\tilde{\alpha}}{2} B_2 - \frac{\tilde{h}}{4} A_1 A_2 B_2 - \frac{\tilde{h}}{8} B_1 (A_2^2 + 3B_2^2) \right] + O(\epsilon^2), \\
A'_2 &= \frac{\epsilon}{\kappa} \left[\left(\frac{\tilde{\omega}_1}{2} - \frac{\tilde{V}_0}{4} \right) B_2 - \frac{3\tilde{g}}{8} B_2 (A_2^2 + B_2^2) - \frac{\tilde{\alpha}}{2} B_1 - \frac{\tilde{h}}{4} A_1 A_2 B_1 - \frac{\tilde{h}}{8} B_2 (A_1^2 + 3B_1^2) \right] + O(\epsilon^2), \\
B'_1 &= \frac{\epsilon}{\kappa} \left[- \left(\frac{\tilde{\omega}_1}{2} + \frac{\tilde{V}_0}{4} \right) A_1 + \frac{3\tilde{g}}{8} A_1 (A_1^2 + B_1^2) + \frac{\tilde{\alpha}}{2} A_2 + \frac{\tilde{h}}{4} A_2 B_1 B_2 + \frac{\tilde{h}}{8} A_1 (3A_2^2 + B_2^2) \right] + O(\epsilon^2), \\
B'_2 &= \frac{\epsilon}{\kappa} \left[- \left(\frac{\tilde{\omega}_1}{2} + \frac{\tilde{V}_0}{4} \right) A_2 + \frac{3\tilde{g}}{8} A_2 (A_2^2 + B_2^2) + \frac{\tilde{\alpha}}{2} A_1 + \frac{\tilde{h}}{4} A_1 B_1 B_2 + \frac{\tilde{h}}{8} A_2 (3A_1^2 + B_1^2) \right] + O(\epsilon^2). \quad (29)
\end{aligned}$$

Equations (29) have three types of equilibria when $\alpha \neq 0$: the trivial one, double modes, and quadruple modes. When $\alpha = 0$, we also find single-mode equilibria and extra double-mode ones. Triple-mode stationary solutions never appear. All the equilibria of Eqs. (29), except for the trivial one, correspond to spatially periodic stationary solutions in the underlying system (18).

There are two kinds of $A_1 A_2$ (double-mode) equilibria. The first satisfies $A_1^2 = A_2^2$, so that the two components have equal amplitudes:

$$\begin{aligned}
(A_1, A_2, B_1, B_2) &= \pm \left(\sqrt{\frac{-4\alpha + 2(2\omega_1 + V_0)}{3(g+h)}}, \sqrt{\frac{-4\alpha + 2(2\omega_1 + V_0)}{3(g+h)}}, 0, 0 \right), \\
(A_1, A_2, B_1, B_2) &= \pm \left(\sqrt{\frac{4\alpha + 2(2\omega_1 + V_0)}{3(g+h)}}, -\sqrt{\frac{4\alpha + 2(2\omega_1 + V_0)}{3(g+h)}}, 0, 0 \right). \quad (30)
\end{aligned}$$

A crucially important issue concerns the dynamical stability of these solutions, which we tested in direct simulations of the underlying equations (5). We found that they are stable, as exemplified in Fig. 1 for $\kappa = \omega = 1$.

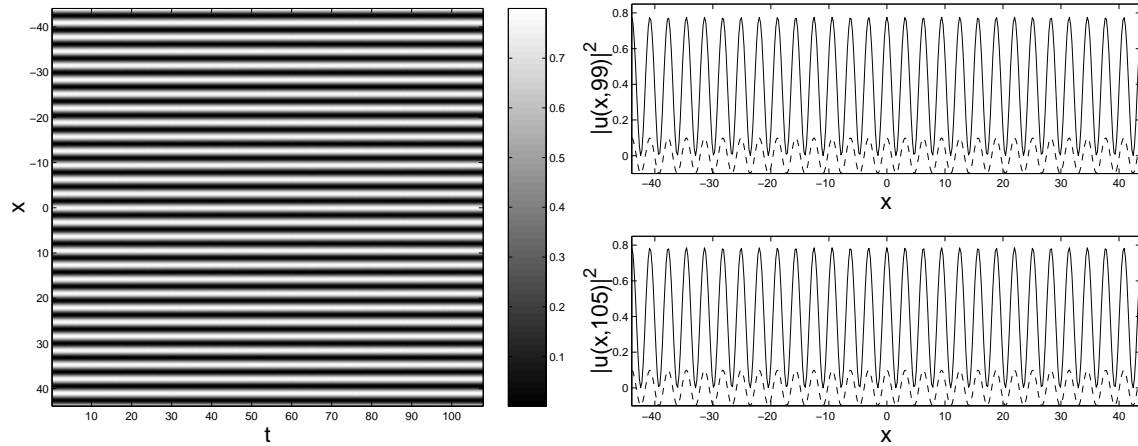


FIG. 1. An example of evolution of the $A_1 A_2$ double mode with *equal* amplitudes $|A_1|$ and $|A_2|$ in the case of the 2 : 1 : 1 subharmonic resonance, constructed as per Eq. (30) for $\kappa = \omega = 1$, $V_0 = 0.1$, $g = h = 0.025$, and $\alpha = 0.02$. The left subplot shows the spatio-temporal evolution of $|\psi_1|^2$ by means of grayscale contour plots ($|\psi_2|^2$ behaves similarly). The right subplot displays snapshots of the field $|\psi_1|^2$ for $t = 99$ (upper panel) and $t = 105$ (lower panel). In the latter panels, the optical-lattice potential is also shown by a dashed line. The results have been obtained through numerical integration of Eqs. (5) in time.

The other $A_1 A_2$ double-mode equilibrium has *unequal* components A_1 and A_2 [note that in the non-resonant case considered above, the equilibria, which are given by Eqs. (25) and by a $\pi/2$ phase shift thereof, always have equal nonzero components]:

$$A_1^2 + A_2^2 = \frac{2(2\omega_1 + V_0)}{3g} > 0,$$

$$(A_1, A_2, B_1, B_2) = \pm \left(\sqrt{\frac{2\omega_1 + V_0}{3g} \pm \frac{1}{3} \sqrt{\frac{(2\omega_1 + V_0)^2}{g^2} - \frac{16\alpha^2}{(g-h)^2}}}, \right. \\ \left. \sqrt{\frac{2\omega_1 + V_0}{3g} \mp \frac{1}{3} \sqrt{\frac{(2\omega_1 + V_0)^2}{g^2} - \frac{16\alpha^2}{(g-h)^2}}}, 0, 0 \right), \quad (31)$$

where the interior + sign in the first component corresponds to the – sign in the second, and vice versa. The exterior sign \pm is independent of the interior one. A necessary condition for the existence of this solution is

$$\left| \frac{2\omega_1 + V_0}{g} \right| \geq \frac{4\alpha}{|g-h|}.$$

In particular, when $h = 2g$, which of special physical relevance (as explained above), the solution becomes

$$(A_1, A_2, B_1, B_2) = \pm \left(\sqrt{\frac{1}{3g} [2\omega_1 + V_0 \pm \sqrt{(2\omega_1 + V_0)^2 - 16\alpha^2}]}, \right. \\ \left. \sqrt{\frac{1}{3g} [2\omega_1 + V_0 \mp \sqrt{(2\omega_1 + V_0)^2 - 16\alpha^2}]}, 0, 0 \right),$$

provided $|2\omega_1 + V_0| \geq 4\alpha$.

In fact, the existence of pairs of equilibria in which the two components have unequal amplitudes that are mirror images of each other is a manifestation of *spontaneous symmetry breaking* in the present model, based on the symmetric system of coupled equations (5). A similar phenomenon was studied in detail (in terms of soliton solutions) in the aforementioned model of dual-core nonlinear optical fibers, which include only the linear coupling between two equations [30].

The stability of the asymmetric stationary solutions, which correspond to equilibria with unequal components, was simulated in the framework of Eqs. (5), a typical example of which is illustrated in Fig. 2. As shown in the figure, all these states are subject to modulational instability, coupled to onset of oscillations between the two components (which is, of course, possible only in the presence of the linear coupling between them).

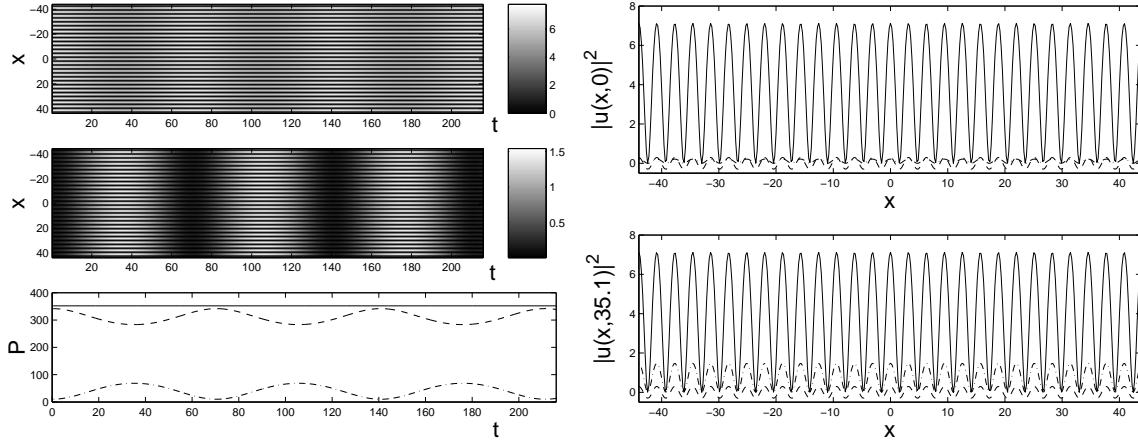


FIG. 2. The same as in Fig. 1, but for the A_1A_2 double mode with *unequal* amplitudes $|A_1|$ and $|A_2|$, given by Eq. (31). The bottom panel in the left subplot shows the time evolution of the numbers of atoms in the two components, $N_{1,2} = \int |u_{1,2}|^2 dx$, by dashed and dash-dotted lines (the sum of the two, $N = N_1 + N_2$, is shown by the solid line). The right panel shows the fields $|\psi_1|^2$ and $|\psi_2|^2$ (by solid and dash-dotted lines, respectively) at $t = 0$ and $t = 75$. The OL potential is shown by the dashed line. The parameters are $g = 0.025$, $h = 0.005$, $\alpha = 0.02$, $V_0 = 0.3$, and $\kappa = \omega = 1$.

There are two types of $B_1 B_2$ dual-mode equilibria. The first satisfies $B_1^2 = B_2^2$ and

$$\begin{aligned} (A_1, A_2, B_1, B_2) &= \pm \left(0, 0, \sqrt{\frac{-4\alpha + 2(2\omega_1 - V_0)}{3(g+h)}}, \sqrt{\frac{-4\alpha + 2(2\omega_1 - V_0)}{3(g+h)}} \right), \\ (A_1, A_2, B_1, B_2) &= \pm \left(0, 0, \sqrt{\frac{4\alpha + 2(2\omega_1 - V_0)}{3(g+h)}}, -\sqrt{\frac{4\alpha + 2(2\omega_1 - V_0)}{3(g+h)}} \right). \end{aligned} \quad (32)$$

The second type satisfies

$$\begin{aligned} B_1^2 + B_2^2 &= \frac{2(2\omega_1 - V_0)}{3g} > 0, \\ (A_1, A_2, B_1, B_2) &= \pm \left(0, 0, \sqrt{\frac{2\omega_1 - V_0}{3g} \pm \frac{1}{3} \sqrt{\frac{(2\omega_1 - V_0)^2}{g^2} - \frac{16\alpha^2}{(g-h)^2}}}, \right. \\ &\quad \left. \sqrt{\frac{2\omega_1 - V_0}{3g} \mp \frac{1}{3} \sqrt{\frac{(2\omega_1 - V_0)^2}{g^2} - \frac{16\alpha^2}{(g-h)^2}}} \right). \end{aligned} \quad (33)$$

As above, the interior + sign in the first component corresponds to the - sign in the second, and vice versa, whereas the exterior \pm is independent. A necessary condition for the existence of this solution is

$$\left| \frac{2\omega_1 - V_0}{g} \right| \geq \frac{4\alpha}{|g-h|}. \quad (34)$$

When $h = 2g$, the present solution becomes

$$\begin{aligned} (A_1, A_2, B_1, B_2) &= \pm \left(0, 0, \sqrt{\frac{1}{3g} \left[2\omega_1 - V_0 \pm \sqrt{(2\omega_1 - V_0)^2 - 16\alpha^2} \right]}, \right. \\ &\quad \left. \sqrt{\frac{1}{3g} \left[2\omega_1 - V_0 \mp \sqrt{(2\omega_1 - V_0)^2 - 16\alpha^2} \right]} \right), \end{aligned}$$

provided $|2\omega_1 - V_0| \geq 4\alpha$.

Unlike in the non-resonant case, the resonant $B_1 B_2$ modes are not precisely phase shifts of the $A_1 A_2$ modes, as the presence of the OL breaks the symmetry that causes this because the resulting parametric excitation in space has only the cosine harmonic. Nevertheless, the equations describing these two classes of modes are similar, differing only in the sign of V_0 .

Direct simulations demonstrate that the stability of stationary solutions corresponding to the $B_1 B_2$ equilibria is the same as in the case of the $A_1 A_2$ double-mode equilibria considered above: the symmetric ones with $|B_1| = |B_2|$ are *stable*, and the asymmetric solutions with $|B_1| \neq |B_2|$ are *unstable*.

We have also found two sets of quadruple modes in the resonant case. The first set satisfies $B_1 = B_2$, $A_1 = -A_2$, and

$$\begin{aligned} A_1^2 &= \frac{V_0}{2h} + \frac{\alpha}{h} + \frac{2\omega_1}{3g+h}, \\ B_1^2 &= -\frac{V_0}{2h} - \frac{\alpha}{h} + \frac{2\omega_1}{3g+h}. \end{aligned}$$

A necessary condition for its existence is

$$\frac{2\omega_1}{3g+h} > \left| \frac{V_0}{2h} + \frac{\alpha}{h} \right|,$$

and hence it is necessary that $\omega_1/(3g+h) > 0$. The second set of quadruple modes satisfies $B_1 = -B_2$, $A_1 = A_2$, and

$$A_1^2 = \frac{V_0}{2h} - \frac{\alpha}{h} + \frac{2\omega_1}{3g+h}, \quad (35)$$

$$B_1^2 = -\frac{V_0}{2h} + \frac{\alpha}{h} + \frac{2\omega_1}{3g+h}. \quad (36)$$

A necessary existence condition here is

$$\frac{2\omega_1}{3g+h} > \left| \frac{V_0}{2h} - \frac{\alpha}{h} \right|,$$

which also implies that $\omega_1/(3g+h) > 0$.

Quadruple modes are considered in the presence of detuning, so that $\omega_1 \neq 0$. This is rather difficult to achieve numerically as it is then necessary that, due to the periodic boundary conditions in x used in the numerical integration scheme, to match *both* the potential and initial condition to the size of the integration domain. Nevertheless, we were able to perform stability simulations in this case too. An example of is shown in Fig. 3. We observe that the quadruple mode is *unstable* against long-wave perturbations that destroy this state, even though the simulation was run for the case of $\alpha = 0$ (no linear coupling). We have not observed stable quadruple states.

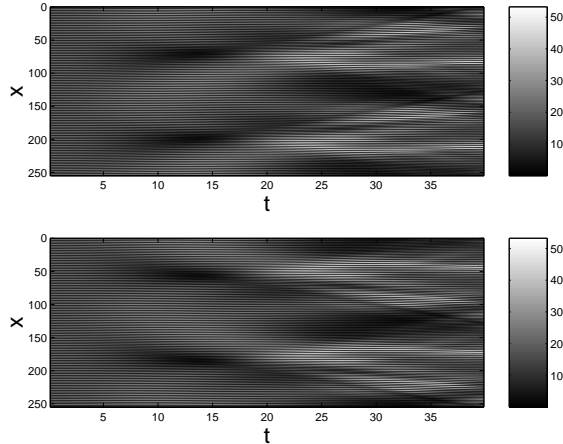


FIG. 3. A typical example of the long-wave instability of a quadruple (four-amplitude) stationary state in the resonant case. The parameters are $\omega = 1.5791$, $\kappa = 1.2320$, $V_0 = 0.1$, $g = 0.025$, $h = 0.05$ and $\alpha = 0$, and the size of the integration box is $L = 255$.

When $\alpha = 0$ (no linear coupling between BEC components), one obtains additional double-mode equilibria and four single-mode equilibria. The latter ones are of the form $(A_1, 0, 0, 0)$, $(0, A_2, 0, 0)$, $(0, 0, B_1, 0)$, $(0, 0, 0, B_2)$, with

$$A_1^2 = A_2^2 = \frac{2(2\omega_1 + V_0)}{3g} > 0,$$

$$B_1^2 = B_2^2 = -\frac{2(2\omega_1 - V_0)}{3g} > 0.$$

The A_j - and B_j -modes both exist when $V_0/g > 0$. In this case ($\alpha = 0$), matter cannot be exchanged between the components. There is also a A_1B_2 double-mode equilibrium [of the form $(A_1, 0, 0, B_2)$], which satisfies

$$A_1^2 = \frac{4\omega_1}{3g+h} + \frac{2V_0}{3g-h} > 0,$$

$$B_2^2 = \frac{4\omega_1}{3g+h} - \frac{2V_0}{3g-h} > 0. \quad (37)$$

From Eq. (37), it follows that a necessary condition for this mode to exist is that $8\omega_1/(3g+h) > 0$. Its counterpart is a A_2B_1 equilibrium in which the subscripts 1 and 2 are swapped in Eq. (37).

One can expand this study to higher-order spatial resonances in BECs either by considering higher-order corrections to the averaged equations, or by employing a perturbative scheme based on elliptic functions, as has been done for single-component BECs in OLs [35,36]. Toward this aim, it may be fruitful to utilize an action-angle formulation and the elliptic function structure of solutions to Eqs. (16) when $V_0 = 0$. However, detailed consideration of higher-order resonances is beyond the scope of this work.

V. CONCLUSIONS

In this work, we analyzed spatial structures in coupled Gross-Pitaevskii (coupled GP) equations, which include both nonlinear and linear interactions, in the optical-lattice (OL) potential. The model describes a BEC consisting of a mixture of two different hyperfine states of one atomic species, which are linearly coupled by a resonant electromagnetic field. In the absence of the OL, we found plane-wave solutions and examined their stability. In the presence of the OL, we derived a system of averaged equations to describe a spatially modulated state which is coupled to the periodic potential through a subharmonic resonance. Equilibria of the latter system were found, and the stabilities of the corresponding spatially periodic solutions to the coupled GP equations were examined using direct simulations. We demonstrated that symmetric dual-mode resonant states with two equal amplitudes are stable, whereas asymmetric ones, with unequal amplitudes, are unstable, generating periodically oscillating solutions. The latter type of dynamical behavior is only possible in the presence of linear coupling between BEC components. Four-mode stationary solutions were found as well, but they were also observed to be unstable.

ACKNOWLEDGEMENTS

We appreciate useful discussions with Richard Rand. P.G.K. gratefully acknowledges support from NSF-DMS-0204585, from the Eppley Foundation for Research and from an NSF-CAREER award. The work of B.A.M. was supported in a part by the grant No. 8006/03 from the Israel Science Foundation.

APPENDIX

The functions F_{A_j} and F_{B_j} , which appear in Eqs. (21), can be written as a sum of harmonic contributions. To simplify the notation, we write \tilde{g} , \tilde{h} , $\tilde{\alpha}$, and \tilde{V}_0 simply as g , h , α , and V .

In the non-resonant case, $F_{A_1} = G_{A_1}/\sqrt{\omega}$, where

$$\begin{aligned}
 G_{A_1}(A_1, A_2, A_3, A_4, x) = & \left[-\frac{\alpha}{2} - \frac{3g}{8}B_1(A_1^2 + B_1^2) - \frac{h}{4}A_1A_2B_2 - \frac{h}{8}B_1(A_2^2 + 3B_2^2) \right] \\
 & + \left[-\frac{\alpha}{2} - \frac{g}{4}A_1(A_1^2 + 3B_1^2) - \frac{h}{2}A_2B_1B_2 - \frac{h}{4}A_1(A_2^2 + B_2^2) \right] \sin(2\sqrt{\omega}x) \\
 & + \left[\frac{g}{8}A_1(3B_1^2 - A_1^2) + \frac{h}{4}A_1B_1B_2 + \frac{h}{8}A_1(B_2^2 - A_2^2) \right] \sin(4\sqrt{\omega}x) \\
 & + \left[-\frac{V}{4}A_1 \right] \sin(2[\kappa - \sqrt{\omega}]x) + \left[\frac{V}{4} \right] \sin(2[\kappa + \sqrt{\omega}]x) \\
 & + \left[\frac{g}{2}B_1^3 + \frac{\alpha}{2}B_2 + \frac{h}{2}B_1B_2^2 \right] \cos(2\sqrt{\omega}x) \\
 & + \left[\frac{g}{8}B_1(3A_1^2 - B_1^2) + \frac{h}{4}A_1A_2B_2 + \frac{h}{8}B_1(A_2^2 - B_2^2) \right] \cos(4\sqrt{\omega}x) \\
 & + \left[\frac{V}{2}B_1 \right] \cos(2\kappa x) + \left[-\frac{V}{4} \right] \cos(2[\kappa - \sqrt{\omega}]x) + \left[-\frac{V}{4} \right] \cos(2[\kappa + \sqrt{\omega}]x), \quad (38)
 \end{aligned}$$

and $F_{B_1} = G_{B_1}/\sqrt{\omega}$, where

$$\begin{aligned}
G_{B_1}(A_1, A_2, A_3, A_4, x) = & \left[\frac{\alpha}{2}A_2 + \frac{3g}{8}A_1(A_1^2 + B_1^2) + \frac{h}{4}A_2B_1B_2 + \frac{h}{8}A_1(A_2^2 + B_2^2) \right] \\
& + \left[\frac{\alpha}{2}B_2 + \frac{g}{4}B_1(3A_1^2 + B_1^2) + \frac{h}{2}A_1A_2B_2 + \frac{h}{4}B_1(A_2^2 + B_2^2) \right] \sin(2\sqrt{\omega}x) \\
& + \left[\frac{g}{8}B_1(3A_1^2 - B_1^2) + \frac{h}{4}A_1A_2B_2 + \frac{h}{8}B_1(A_2^2 - B_2^2) \right] \sin(4\sqrt{\omega}x) \\
& + \left[\frac{V}{4}B_1 \right] \sin(2[\kappa - \sqrt{\omega}]x) + \left[-\frac{V}{4} \right] \sin(2[\kappa + \sqrt{\omega}]x) \\
& + \left[\frac{\alpha}{2}A_2 + \frac{g}{2}A_1^3 + \frac{h}{2}A_1A_2^2 \right] \cos(2\sqrt{\omega}x) \\
& + \left[\frac{g}{8}A_1(A_1^2 - 3B_1^2) - \frac{h}{4}A_2B_1B_2 + \frac{h}{8}A_1(A_2^2 - B_2^2) \right] \cos(4\sqrt{\omega}x) \\
& + \left[-\frac{V}{2}A_1 \right] \cos(2\kappa x) + \left[-\frac{V}{4}A_1 \right] \cos(2[\kappa - \sqrt{\omega}]x) + \left[-\frac{V}{4}A_1 \right] \cos(2[\kappa + \sqrt{\omega}]x) \quad (39)
\end{aligned}$$

Only the $O(1)$ terms remain after averaging.

In the resonant case, one obtains, after averaging, an extra term depending on V , because a term that was a prefactor of a non-constant harmonic in (38) and (39) has become a coefficient in front of the $O(1)$ term. Other harmonic terms are also simplified due to the resonance, but they nevertheless do not contribute to the averaged equations because they are still prefactors in front of non-constant harmonics. The extra terms with ω_1 arise from Taylor expanding in ϵ and keeping the leading-order terms. In the resonant case, $F_{A_1} = G_{A_1}/\kappa$ and $F_{B_1} = G_{B_1}/\kappa$.

In both the resonant and non-resonant cases, the expressions for F_{A_2} and F_{B_2} are obtained by switching the subscripts $1 \leftrightarrow 2$ in the equations above.

- [1] G. P. Agrawal. *Nonlinear Fiber Optics*. Academic Press, San Diego, CA, 1995.
- [2] G. L. Alfimov, P. G. Kevrekidis, V. V. Konotop, and M. Salerno. Wannier functions analysis of the nonlinear Schrodinger equation with a periodic potential. *Physical Review E*, 66(046608), October 2002.
- [3] B. P. Anderson and M. A. Kasevich. Macroscopic quantum interference from atomic tunnel arrays. *Science*, 282(5394):1686–1689, November 1998.
- [4] B. B. Baizakov, V. V. Konotop, and M. Salerno. Regular spatial structures in arrays of Bose-Einstein condensates induced by modulational instability. *Journal of Physics B: Atomic Molecular and Optical Physics*, 35:5105–5119, 2002.
- [5] Y. B. Band, I. Towers, and Boris A. Malomed. Unified semiclassical approximation for Bose-Einstein condensates: Application to a BEC in an optical potential. *Physical Review A*, 67(023602), February 2003.
- [6] Kirstine Berg-Sørensen and Klaus Mølmer. Bose-Einstein condensates in spatially periodic potentials. *Physical Review A*, 58(2):1480–1484, August 1998.
- [7] Jared C. Bronski, Lincoln D. Carr, Ricardo Carretero-González, Bernard Deconinck, J. Nathan Kutz, and Keith Promislow. Stability of attractive Bose-Einstein condensates in a periodic potential. *Physical Review E*, 64(056615):1–11, 2001.
- [8] Jared C. Bronski, Lincoln D. Carr, Bernard Deconinck, and J. Nathan Kutz. Bose-Einstein condensates in standing waves: The cubic nonlinear Schrödinger equation with a periodic potential. *Physical Review Letters*, 86(8):1402–1405, February 2001.
- [9] Jared C. Bronski, Lincoln D. Carr, Bernard Deconinck, J. Nathan Kutz, and Keith Promislow. Stability of repulsive Bose-Einstein condensates in a periodic potential. *Physical Review E*, 63(036612):1–11, 2001.
- [10] S. Burger, F. S. Cataliotti, C. Fort, F. Minardi, and M. Inguscio. Superfluid and dissipative dynamics of a Bose-Einstein condensate in a periodic optical potential. *Physical Review Letters*, 86(20):4447–4450, May 2001.
- [11] Keith Burnett, Mark Edwards, and Charles W. Clark. The theory of Bose-Einstein condensation of dilute gases. *Physics Today*, 52(12):37–42, December 1999.
- [12] Th. Busch, J. I. Cirac, V. M. Pérez-García, and P. Zoller. Stability and collective excitations of a two-component Bose-Einstein condensed gas: A moment approach. *Physical Review A*, 56(4):2978–2983, October 1997.
- [13] Ricardo Carretero-González and Keith Promislow. Localized breathing oscillations of Bose-Einstein condensates in periodic traps. *Physical Review A*, 66(033610), September 2002.

- [14] F. S. Cataliotti, L. Fallani, F. Ferlaino, C. Fort, P. Maddaloni, and M. Inguscio. Superfluid current disruption in a chain of weakly coupled Bose-Einstein condensates. *New Journal of Physics*, 5:71.1–71.7, June 2003.
- [15] Dae-Il Choi and Qian Niu. Bose-Einstein condensates in an optical lattice. *Physical Review Letters*, 82(10):2022–2025, March 1999.
- [16] Franco Dalfovo, Stefano Giorgini, Lev P. Pitaevskii, and Sandro Stringari. Theory of Bose-Einstein condensation on trapped gases. *Reviews of Modern Physics*, 71(3):463–512, April 1999.
- [17] Bernard Deconinck, B. A. Frigiyik, and J. Nathan Kutz. Dynamics and stability of Bose-Einstein condensates: The nonlinear Schrödinger equation with periodic potential. *Journal of Nonlinear Science*, 12(3):169–205, 2002.
- [18] Bernard Deconinck, J. Nathan Kutz, Matthew S. Patterson, and Brandon W. Warner. Dynamics of periodic multi-component Bose-Einstein condensates. *Journal of Physics A—Mathematics and General*, 36(20):5431–5447, May 2003.
- [19] B. D. Esry, Chris H. Greene, James P. Burke Jr., and John L. Bohn. Hartree-Fock theory for double condensates. *Physical Review Letters*, 78(19):3594–3597, May 1997.
- [20] John Guckenheimer and Philip Holmes. *Nonlinear Oscillations, Dynamical Systems, and Bifurcations of Vector Fields*. Number 42 in Applied Mathematical Sciences. Springer-Verlag, New York, NY, 1983.
- [21] E. W. Hagley, L. Deng, M. Kozuma, J. Wen, K. Helmerson, S. L. Rolston, and W. D. Phillips. A well-collimated quasi-continuous atom laser. *Science*, 283(5408):1706–1709, March 1999.
- [22] Tin-Lun Ho and V. B. Shenoy. Binary mixtures of Bose condensates of alkali atoms. *Physical Review Letters*, 77(16):3276–3279, October 1996.
- [23] S. Inouye, M. R. Andrews, J. Stenger, H. J. Miesner, D. M. Stamper-Kurn, and W. Ketterle. Observation of Feshbach resonances in a Bose-Einstein condensate. *Nature*, 392(6672):151–154, March 1998.
- [24] Wolfgang Ketterle. Experimental studies of Bose-Einstein condensates. *Physics Today*, 52(12):30–35, December 1999.
- [25] Thorsten Köhler. Three-body problem in a dilute Bose-Einstein condensate. *Physical Review Letters*, 89(21):210404, 2002.
- [26] Pearl J. Y. Louis, Elena A. Ostrovskaya, Craig M. Savage, and Yuri S. Kivshar. Bose-einstein condensates in optical lattices: Band-gap structure and solitons. *Physics Review A*, 67(013602), 2003.
- [27] M. Machholm, A. Nicolin, C. J. Pethick, and H. Smith. Spatial period-doubling in Bose-Einstein condensates in an optical lattice. ArXiv:cond-mat/0307183v1, July 2003.
- [28] M. Machholm, C. J. Pethick, and H. Smith. Band structure, elementary excitations, and stability of a Bose-Einstein condensate in a periodic potential. *Physical Review A*, 67:053613–1–15, 2003.
- [29] Boris A. Malomed. Polarization dynamics and interactions of solitons in a birefringent optical fiber. *Physical Review A*, 43(1):410, January 1991.
- [30] Boris A. Malomed, I. M. Skinner, P. L. Chu, and G. D. Peng. Symmetric and asymmetric solitons in twin-core nonlinear optical fibers. *Physical Review E*, 53(4):4084, April 1996.
- [31] Boris A. Malomed, Z. H. Wang, P. L. Chu, and G. D. Peng. Multichannel switchable system for spatial solitons. *Journal of the Optical Society of America B*, 16(8):1197–1203, August 1999.
- [32] Erich J. Mueller. Superfluidity and mean-field energy loops; hysteretic behavior in Bose-Einstein condensates. *Physical Review A*, 66:063603–1–11, 2002.
- [33] C. J. Myatt, E. A. Burt, R. W. Ghrist, E. A. Cornell, and C. E. Wieman. Production of two overlapping Bose-Einstein condensates by sympathetic cooling. *Physical Review Letters*, 78:586–589, January 1997.
- [34] C. J. Pethick and H. Smith. *Bose-Einstein Condensation in Dilute Gases*. Cambridge University Press, Cambridge, United Kingdom, 2002.
- [35] Mason A. Porter and Predrag Cvitanović. A perturbative analysis of modulated amplitude waves in Bose-Einstein condensates. ArXiv: nlin.CD/0308024, Submitted, August 2003.
- [36] Mason A. Porter and Predrag Cvitanović. Modulated amplitude waves in Bose-Einstein condensates. *Physical Review E*, To appear. ArXiv: nlin.CD/0307032.
- [37] H. Pu and N. P. Bigelow. Collective excitations, metastability, and nonlinear response of a trapped two-species Bose-Einstein condensate. *Physical Review Letters*, 80(6):1134–1137, February 1998.
- [38] H. Pu and N. P. Bigelow. Properties of two-species Bose condensates. *Physical Review Letters*, 80(6):1130–1133, February 1998.
- [39] Richard H. Rand. *Topics in Nonlinear Dynamics with Computer Algebra*, volume 1 of *Computation in Education: Mathematics, Science and Engineering*. Gordon and Breach Science Publishers, USA, 1994.
- [40] Richard H. Rand. Dynamics of a nonlinear parametrically-excited pde: 2-term truncation. *Mechanics Research Communications*, 23(3):283–289, 1996.
- [41] Richard H. Rand. Lecture notes on nonlinear vibrations. a free online book available at <http://www.tam.cornell.edu/randdocs/nlvibe45.pdf>, 2003.
- [42] L. Salasnich, A. Parola, and L. Reatto. Periodic quantum tunnelling and parametric resonance with cigar-shaped Bose-Einstein condensates. *Journal of Physics B: Atomic Molecular and Optical Physics*, 35(14):3205–3216, July 2002.
- [43] Marek Trippenbach, Krzysztof Góral, Kazimierz Rzążewski, Boris Malomed, and Y. B. Band. Structure of binary Bose-Einstein condensates. *Journal of Physics B: Atomic, Molecular, and Optical Physics*, 33:4017–4031, 2000.
- [44] A. Trombettoni and A. Smerzi. Discrete solitons and breathers with dilute Bose-Einstein condensates. *Physical Review Letters*, 86(11):2353–2356, March 2001.
- [45] J. A. C. Weideman and B. M. Herbst. Split-step methods for the solution of the nonlinear Schrödinger equation. *SIAM*

Journal on Numerical Analysis, 23(3):485–507, June 1986.

- [46] Biao Wu, Roberto B. Diener, and Qian Niu. Bloch waves and Bloch Bands of Bose-Einstein condensates in optical lattices. *Physical Review A*, 65:025601–1–4, 2002.